arXiv:1403.5948v2 [math.NA] 25 Mar 2014

Analysis and discretization of the volume penalized Laplace operator with Neumann boundary conditions

Dmitry Kolomenskiy[a], Romain Nguyen van yen[b], Kai Schneider[c]

[a]*Department of Mathematics and Statistics, McGill University, CRM, Montréal, Canada*
[b]*FB Mathematik und Informatik, Freie Universität Berlin, Germany*
[c]*M2P2-CNRS, Aix-Marseille Université, 38 rue Joliot-Curie, 13451 Marseille Cedex 20, France*

Abstract

We study the properties of an approximation of the Laplace operator with Neumann boundary conditions using volume penalization. For the one-dimensional Poisson equation we compute explicitly the exact solution of the penalized equation and quantify the penalization error. Numerical simulations using finite differences allow then to assess the discretisation and penalization errors. The eigenvalue problem of the penalized Laplace operator with Neumann boundary conditions is also studied. As examples in two space dimensions, we consider a Poisson equation with Neumann boundary conditions in rectangular and circular domains.

Keywords:
Volume penalization, Neumann boundary conditions, Laplace operator, Poisson equation

1. Introduction

Solving partial differential equations (PDEs) in complex domains is unavoidable in real world applications. Different numerical methods have been developed so far, for example body fitted computational grids or coordinate transforms [4]. Immersed boundary methods are still of growing interest due to their high flexibility and their ease of implementation into existing codes. The underlying idea of these methods is to embed the complex geometry into a simple geometry (*e.g.* a rectangle) for which efficient solvers are available. The boundary conditions are then imposed by adding supplementary terms to the governing equations. Different penalization approaches are on

the market, for example, surface and volume penalization techniques, immersed boundary methods using direct forcing and Lagrangian multipliers. For reviews on immersed boundary techniques, we refer to [13, 10].

In the current work, we focus on the volume penalization method developed by Angot *et al.* [1] for imposing Dirichlet boundary conditions in viscous fluid flow. Physically, the boundary conditions correspond to no-slip conditions on the wall, *i.e.*, both the normal and the tangential velocity do vanish at the fixed wall. This penalization approach is physically motivated as walls or solid obstacles are modeled as porous media whose permeability tends to zero. Mathematically, it has also been justified. In [1, 3] it was shown that the solution of the penalized Navier–Stokes equations converges towards the solution of the Navier–Stokes equations with no-slip boundary conditions, while the error depends on the penalization parameter. Various applications of the volume penalization method to impose Dirichlet boundary conditions can be found in the literature. Briefly summarizing, we can mention computations of confined hydrodynamic and magnetohydrodynamic turbulence, which can be found in [17] and [18, 11], respectively. Fluid-structure interaction simulations have been carried out for moving obstacles [6] and for flexible beams [8]. Applications to the aerodynamics of insect flight in two and three space dimensions can be found in [7].

Most of the developed penalization techniques deal with Dirichlet boundary conditions, and only few allow to impose Neumann conditions. Neumann boundary conditions in partial differential equations are encountered in many applications, for example when solving the Poisson equation for pressure in incompressible flows, to model adiabatic walls in heat transfer, or to impose no-flux conditions for passive or reactive scalars at walls. In [2] a review on the pure Neumann problem using finite elements is given and different techniques for solving the algebraic system are discussed. An extension of the volume penalization method [1] to impose Neumann or Robin boundary conditions has been presented in [14] and applied in the context of finite element or finite volumes [15]. In [5] we extended this method for pseudo-spectral discretizations and applied it to scalar mixing in incompressible flow for fixed and also for moving geometries imposing no-slip conditions for the velocity and no-flux conditions for the passive scalar field.

The fields of possible applications of the volume penalization method for imposing Neumann conditions in complex geometries are multifarious and large. For example, confined magnetohydrodynamic flow configurations can be studied imposing finite values of the current density at the wall, or

convection problems which necessitate imposing a given heat flux at the boundary.

Motivated by the work of [9], where the properties of Fourier approximations of elliptic problems with discontinuous coefficients have been studied, we analyzed mathematically the penalized Laplace and Stokes operators with Dirichlet boundary conditions in [12] and verified the predicted convergence numerically. The aim of the present work is to generalize the approach developed in [12] and to analyze the penalized Laplace operator with Neumann boundary conditions. For a one-dimensional Poisson equation, we explicitely compute the penalization error by solving the penalized equation analytically. Discretizing the penalized equation using finite difference methods, we study the influences of both the numerical resolution and the value of the penalization parameter.

The outline of the paper is the following: First we consider the penalized Poisson equation in one space dimension with Neumann boundary conditions both analytically and numerically. Then, in section 3 we study the eigenvalue problem of the penalized Laplace operator. Section 4 presents applications of the penalization method to solve the Poisson equation in two dimensions in a rectangular and a circular domain. Finally, some conclusions are drawn and some perspectives are given in section 5.

2. Poisson equation with Neumann boundary conditions and penalization

2.1. Problem setting

We consider the one-dimensional Poisson equation

$$-w'' = f \quad \text{for} \quad x \in (0, \pi) \tag{1}$$

completed with homogeneous Neumann boundary conditions, $w'(x = 0) = w'(x = \pi) = 0$ and for $f(x) = m^2 \cos mx$, $m \in \mathbb{Z}$. The exact solution $w \in H^2(0, \pi)$ is given by $w(x) = \cos mx + C$, where $C \in R$ is an arbitrary constant, as the solution is not unique. Integrating eq. (1) over $(0, \pi)$ yields the compatibility condition $\int_0^\pi f(x)dx = w'(x = \pi) - w'(x = 0) = 0$ which has to be satisfied to guarantee the existence of a solution.

Following [5], the penalized Poisson equation reads

$$-d_x((1 - \chi) + \eta\chi)d_x v = f \quad \text{for} \quad x \in (0, 2\pi) \tag{2}$$

where $\eta > 0$ is the penalization parameter and χ the mask function defined by

$$\chi(x) = \begin{cases} 0 & \text{for} \quad 0 < x < \pi \\ 1/2 & \text{for} \quad x = 0 \text{ or } x = \pi \\ 1 & \text{elsewhere} \end{cases} \tag{3}$$

The domain $\Omega_f =]0, \pi[$, also called fluid domain, is imbedded into the larger domain $\Omega =]0, 2\pi[$ imposing now periodic boundary conditions at the boundary. Thus we have $\Omega = \Omega_f \cup \Omega_s$, where Ω_s is the penalization domain, also called solid domain.

2.2. Analytic solution of the one-dimensional penalized equation

The penalized Poisson equation (2) can be solved analytically in each sub-domain, i.e.,

$$-v'' = f \quad \text{for} \quad x \in]0, \pi[\tag{4}$$

$$-\eta v'' = 0 \quad \text{for} \quad x \in]\pi, 2\pi[\tag{5}$$

and accordingly we obtain

$$v(x) = \begin{cases} \cos mx + A_1 x + A_2 & \text{for} \quad x \in]0, \pi[\\ B_1 x + B_2 & \text{for} \quad x \in]\pi, 2\pi[\end{cases} \tag{6}$$

The coefficients can then be determined by imposing continuity of the solution and of the flux, at $x = 0 (= 2\pi)$ and π,

$$v(\pi^-) = v(\pi^+) \quad \text{and} \quad v(0^+) = v(2\pi^-) \tag{7}$$

$$v'(\pi^-) = \eta v'(\pi^+) \quad \text{and} \quad v'(0^+) = \eta v'(2\pi^-) \tag{8}$$

This results in

$$A_1 = \frac{1 - (-1)^m}{\pi(1 + 1/\eta)} \quad \text{and} \quad B_1 = \frac{1}{\eta} A_1 \tag{9}$$

$$A_2 = \frac{2\pi}{\eta} \frac{1 - (-1)^m}{\pi(1 + 1/\eta)} - 1 + B_2 \tag{10}$$

Only three of the four coefficients can be determined, B_2 corresponds to the additive constant.

Figure 1 shows the exact solution, $w(x)$, and the solution of the penalized problem, $v(x)$ (for $\eta = 10^{-1}$), in the case $m = 1$. Unlike for the penalized heat

equation with Neumann boundary conditions [5], here there is no boundary layer in the penalized domain. Note that, if m is even, v and w coincide exactly. Therefore, in the following let us assume m odd. The coefficients of the penalized solution become (with the integration constant chosen such as to ensure zero mean value)

$$A_1 = \frac{2}{\pi}\frac{\eta}{1+\eta}, \qquad B_1 = \frac{2}{\pi}\frac{1}{1+\eta}, \qquad A_2 = -\frac{\eta}{1+\eta}, \qquad B_2 = -\frac{3}{1+\eta}. \tag{11}$$

The difference between the exact solution of the non penalized problem w and v yields the penalization error $||w(x) - v(x)||$ which is of order $O(\eta)$ in Ω_f, and which is in this particular case better than the general $O(\sqrt{\eta})$ convergence behavior shown in [5] for the heat equation.

It is straightforward to compute the Fourier coefficients of the solution of the penalized equation $v(x)$:

$$\hat{v}(k) \;=\; \begin{cases} \dfrac{i}{\pi}\dfrac{m^2}{k(m^2-k^2)} & \text{if } k \text{ even} \\ \dfrac{2}{\pi^2 k^2}\dfrac{1-\eta}{1+\eta} & \text{if } k \text{ odd and } k \neq \pm m \\ \dfrac{2}{\pi^2 m^2}\dfrac{1-\eta}{1+\eta} + \dfrac{1}{4} & \text{if } k \text{ odd and } k = \pm m \end{cases} \tag{12}$$

Figure 2 displays the decay of the absolute value of $\hat{v}$. The leading order is $\sim k^{-2}$ and the constant pre-factor is finite in the limit $\eta \to 0$. There is no 'intermediate' regime of slow decay at low k, because there is no boundary layer in contrast to the Dirichlet case [12]. This rate of decay of $\hat{v}$ suggests that a Galerkin truncated approximation to v converges as $N^{-3/2}$.

2.3. Discretization error of the second order finite difference scheme

Now we consider the discretization of the penalized equation using centered finite differences of second order. Discretizing the equation

$$-\, d_x(\theta(x)) d_x u \;=\; f \quad \text{for} \quad x \in (0, 2\pi) \tag{13}$$

where $\theta = (1-\chi) + \eta\chi$ with periodic boundary conditions on N grid points $x_i = i/(2\pi), i = 0, ..., N-1$ yields to the following linear system

$$-\, D\Theta D = F \tag{14}$$

where D is the first derivative matrix (Toeplitz) and $\Theta = [\theta(x_0), \theta(x_1), ..., \theta(x_{N-1})]$ with $\theta(x_i) = 1 - \chi(x_i) + \eta\chi(x_i))$ and $F = [f(x_0), f(x_1), ..., f(x_{N-1})]$ are vectors in $\mathbb{R}^N$.

The matrix $A = -D\Theta(x)D$ is singular (it has an eigenvalue 0) and a solution only exists if F is in the image of A. For solving the linear system thus special care has to be taken using either the pseudoinverse, or removing one equation. This point will be addressed later.

The penalized differential operator can then be approximated to the second order accuracy with the following finite-difference scheme:

$$A = -\frac{1}{2}\left(D_F\Theta(x)D_B + D_B\Theta(x)D_F\right), \tag{15}$$

where D_B and D_F are the backward and forward first derivative matrices,

$$D_B = \frac{1}{h}\begin{pmatrix} 1 & & & -1 \\ -1 & 1 & & \\ & & \ddots & \\ & & -1 & 1 \end{pmatrix}, \qquad D_F = \frac{1}{h}\begin{pmatrix} -1 & 1 & & \\ & -1 & 1 & \\ & & & \ddots \\ 1 & & & -1 \end{pmatrix} \tag{16}$$

where $h = 2\pi/N$. Note that $dim\ ker(A) = 1$ reflecting the fact that the (periodic) solution is defined up to an additive constant. We fix this constant by imposing the mean value to be zero,

$$F_1 = 0, \quad A_{1,j} = 1, \quad j = 1, ..., N, \tag{17}$$

where $N = dim(A)$. This yields an invertible matrix. Figure 3 confirms the second-order rate of convergence, provided that η is sufficiently small.

Note that we found that defining the mask function (eq. 3) using either the value 0 or 1 at the interface, instead of 1/2, yields very similar results.

3. Eigenvalue problem of the penalized Laplace operator

3.1. Exact eigenvalue problem

Now we consider the eigenvalue problem of the Laplace operator with homogeneous Neumann boundary conditions,

$$-\psi'' = \lambda\psi \qquad x \in (0, \pi) \tag{18}$$

with $\psi'(0) = \psi'(\pi) = 0$. The resulting eigenfunctions are $\psi_n(x) = \cos(nx)$ for $n \in \mathbb{N}$ and the corresponding eigenvalues are given by $\lambda_n = n^2$. Typically, the eigenfunctions are normalized with respect to the L^2 norm and thus the factor $\sqrt{2/\pi}$ has to be included and for $n = 0$ we have $\psi_0 = 1/\sqrt{\pi}$.

3.2. Penalized eigenvalue problem

The eigenvalue problem of the penalized Laplace operator with homogeneous Neumann boundary conditions reads,

$$\begin{aligned} -\phi'' &= \lambda\phi \qquad \text{for} \quad x \in]0,\pi[&& (19)\\ -\eta\phi'' &= \lambda\phi \quad \text{for} \quad x \in]\pi,2\pi[&& (20) \end{aligned}$$

where $\eta > 0$ and periodic boundary conditions are imposed at 0 and 2π. Imposing continuity of the solution and of the flux, the problem can be solved exactly and we obtain the eigenfunctions

$$\phi(x) = \begin{cases} A_1\cos(\sqrt{\lambda}x) + B_1\sin(\sqrt{\lambda}x) & \text{for} \quad 0 < x < \pi \\ A_2\cos(\sqrt{\lambda/\eta}x) + B_2\sin(\sqrt{\lambda/\eta}x) & \text{for} \quad \pi < x < 2\pi \end{cases} \tag{21}$$

where the coefficients are given by solving the linear system

$$A_1\cos(\sqrt{\lambda}\pi^-) + B_1\sin(\sqrt{\lambda}\pi^-) = A_2\cos(\sqrt{\lambda/\eta}\pi^+) + B_2\sin(\sqrt{\lambda/\eta}\pi^+) \tag{22}$$

$$-A_1\sin(\sqrt{\lambda}\pi^-) + B_1\cos(\sqrt{\lambda}\pi^-) = -A_2\sqrt{\eta}\sin(\sqrt{\lambda/\eta}\pi^+) + B_2\sqrt{\eta}\cos(\sqrt{\lambda/\eta}\pi^+) \tag{23}$$

$$A_1\cos(\sqrt{\lambda}0^+) + B_1\sin(\sqrt{\lambda}0^+) = A_2\cos(\sqrt{\lambda/\eta}2\pi^-) + B_2\sin(\sqrt{\lambda/\eta}2\pi^-) \tag{24}$$

$$-A_1\sin(\sqrt{\lambda}0^+) + B_1\cos(\sqrt{\lambda}0^+) = -A_2\sqrt{\eta}\sin(\sqrt{\lambda/\eta}2\pi^-) + B_2\sqrt{\eta}\cos(\sqrt{\lambda/\eta}2\pi^-) \tag{25}$$

The coefficients A_1 and B_1 can be eliminated and we obtain a homogeneous linear system for the coefficients A_2 and B_2.

$$\begin{pmatrix} a & b \\ c & d \end{pmatrix} \begin{pmatrix} A_2 \\ B_2 \end{pmatrix} = \begin{pmatrix} 0 \\ 0 \end{pmatrix} \tag{26}$$

with coefficients

$$a = \cos(\sqrt{\lambda/\eta}2\pi^-)\cos(\sqrt{\lambda}\pi^-) - \sqrt{\eta}\sin(\sqrt{\lambda/\eta}2\pi^)\sin(\sqrt{\lambda}\pi^-) - \cos(\sqrt{\lambda/\eta}\pi^+) \tag{27}$$

$$b = \sin(\sqrt{\lambda/\eta}2\pi^-)\cos(\sqrt{\lambda}\pi^-) + \sqrt{\eta}\cos(\sqrt{\lambda/\eta}2\pi^)\sin(\sqrt{\lambda}\pi^-) - \sin(\sqrt{\lambda/\eta}\pi^+) \tag{28}$$

$$c = -\cos(\sqrt{\lambda/\eta}2\pi^-)\sin(\sqrt{\lambda}\pi^-) - \sqrt{\eta}\sin(\sqrt{\lambda/\eta}2\pi^)\cos(\sqrt{\lambda}\pi^-) + \sqrt{\eta}\sin(\sqrt{\lambda/\eta}\pi^+) \tag{29}$$

$$d = -\sin(\sqrt{\lambda/\eta}2\pi^-)\sin(\sqrt{\lambda}\pi^-) + \sqrt{\eta}\cos(\sqrt{\lambda/\eta}2\pi^)\cos(\sqrt{\lambda}\pi^-) - \sqrt{\eta}\cos(\sqrt{\lambda/\eta}\pi^+) \tag{30}$$

The eigenvalues λ can then be determined by computing the zeros of the determinant of the linear system, *i.e.*, solving the nonlinear equation

$$G(\lambda;\eta) \;=\; ad - bc \;=\; 0 \tag{31}$$

for a given value of η. We did not succeed solving this system symbolically for arbitrary η, but we can make the following observations:

- The function G is a periodic function in $\sqrt{\lambda/\eta}$.
- The value $\lambda = 0$ is a solution of eq.(31) and thus an eigenvalue of the penalized operator.
- The values $\lambda = i^2$ and $\lambda = \eta i^2$ for $i \in \mathbb{N}$ play a special role as different terms in eq.(31) vanish.
- For the special choice of the penalization parameter $\eta = i^2/j^2$ with $i, j \in \mathbb{N}$, we have explicit solutions and the eigenvalues are $\lambda = i^2$ and $\lambda = \eta i^2$, for $i \in \mathbb{N}$.

The above findings motivate the fact that $\lambda = i^2$ and $\lambda = \eta i^2$ are indeed good approximations of the zeros of G for general values of $\eta \in \mathbb{R}^+$.

3.3. Numerical solution of the penalized eigenvalue problem

The penalized eigenvalue problem is now solved numerically using second order finite differences. Thus we discretize,

$$-\, d_x(\theta(x))d_x u \;=\; \lambda u \quad \text{for} \quad x \in (0, 2\pi) \tag{32}$$

using eq. (15) where periodic boundary conditions are imposed at 0 and 2π. The operator $-d_x(\theta(x))d_x$ is self-adjoint and semi-positive definite, hence all eigenvalues λ are real and positive.

The finite-difference penalized Laplace operator has also a zero eigenvalue, since the solution of the boundary-value problem is only defined up to an additive constant. One can also identify eigenfunctions of the penalized problem that correspond to the eigenmodes of the original boundary-value problem. Three of them are displayed in figure 4. They correspond to eigenvalues number $N/2$, $N/2+1$ and $N/2+2$. In the fluid domain (or physical domain, or low-diffusivity domain) they behave like $\cos nx$, and they are close to zero in the other half of the domain. Similar eigenfunctions exist in

the solid (fictitious domain, or large-diffusivity domain), they correspond to the largest eigenvalues. All non-zero eigenvalues sorted by their magnitude, in the accending order, are shown in figure 5 for three choices of the model parameters: $N = 512$, $\eta = 10^{-3}$, $N = 128$, $\eta = 10^{-8}$ and $N = 512$, $\eta = 10^{-8}$. The spectrum λ_i changes from an ηi^2 power law to a concave function approximately at $i = N/2$ (figure 5, left). Applying a shift ($i' = i - N/2 + 2$) and replotting the upper half of the spectrum for $i \geq N/2 - 1$ shows again a power law behavior $\propto i^2$ as illustrated in (figure 5, right). For increasing resolution N, we can observe that these eigenvalues in the upper half of the spectrum do indeed converge versus the eigenvalues of the non-penalized Laplace operator given by i^2. The eigenvalues in the lower part of the spectrum depend on the penalization parameter η and do converge to zero for $\eta \to 0$.

The upper half of the spectrum corresponds to the modes that are only non-trivial in either part of the domain (despite some small oscillations), like in figure 5. The lower half of the spectrum corresponds to modes that oscillate with the grid frequency in either subdomain. Figure 6 shows the decay of the distance between the eigenfunctions of the discrete penalized operator (like those in figure 4) and their exact counterparts, as h decreases. In this example, the penalization parameter $\eta = 10^{-8}$ is sufficiently small so that the penalization error is smaller than the discretization error within the range of h shown in the figure. These computations suggest that the discrete eigenfunctions considered here are only a first-order approximation to those of the original boundary-value problem, whereas (we remind that) the solution to the Poisson equation is second-order accurate in h.

4. Application to the penalized Poisson equation in 2d

Now, we consider a Poisson equation in two space dimensions complemented with homogeneous Neumann boundary conditions,

$$-\nabla^2 u = f$$

with $\partial_n u = 0$. First, we consider a square domain and then a circular domain.

The two-dimensional penalized equation in Cartesian coordinates reads

$$-\partial_x(\theta(x,y)\partial_x u(x,y)) - \partial_y(\theta(x,y)\partial_y u(x,y)) = f(x,y). \tag{33}$$

The partial derivatives are approximated using the same second order finite-difference scheme that led to (15).

Let us first consider an example in which the interface is aligned with the grid. The computational domain is a periodization of a square $\Omega = [0, 2\pi] \times [0, 2\pi]$, and the fluid occupies a smaller square sub-domain, $\Omega_f = [\pi/2, 3\pi/2] \times [\pi/2, 3\pi/2]$. Thus, the mask function is

$$\chi(x,y) = \begin{cases} 0 & \text{if } x \in]\frac{\pi}{2}, \frac{3\pi}{2}[\text{ and } y \in]\frac{\pi}{2}, \frac{3\pi}{2}[; \\ \frac{1}{2} & \text{if } x = \frac{\pi}{2}, y \in]\frac{\pi}{2}, \frac{3\pi}{2}[\text{ or } x = \frac{3\pi}{2}, y \in]\frac{\pi}{2}, \frac{3\pi}{2}[\\ & \quad \text{or } y = \frac{\pi}{2}, x \in]\frac{\pi}{2}, \frac{3\pi}{2}[\text{ or } y = \frac{3\pi}{2}, x \in]\frac{\pi}{2}, \frac{3\pi}{2}[; \\ \frac{1}{4} & \text{if } x = \frac{\pi}{2}, y = \frac{\pi}{2} \text{ or } x = \frac{3\pi}{2}, y = \frac{\pi}{2} \\ & \quad \text{or } x = \frac{\pi}{2}, y = \frac{3\pi}{2} \text{ or } x = \frac{3\pi}{2}, y = \frac{3\pi}{2}; \\ 1 & \text{otherwise} \end{cases} \tag{34}$$

Let the right-hand side of the penalized Poisson equation (33) be

$$f(x,y) = \begin{cases} 5 \sin x \cos 2y & \text{if } x \in]\frac{\pi}{2}, \frac{3\pi}{2}[\text{ and } y \in]\frac{\pi}{2}, \frac{3\pi}{2}[; \\ \frac{5}{2} \cos 2y & \text{if } x = \frac{\pi}{2}, y \in]\frac{\pi}{2}, \frac{3\pi}{2}[; \\ -\frac{5}{2} \cos 2y & \text{if } x = \frac{3\pi}{2}, y \in]\frac{\pi}{2}, \frac{3\pi}{2}[; \\ -\frac{5}{2} \sin x & \text{if } y = \frac{\pi}{2}, x \in]\frac{\pi}{2}, \frac{3\pi}{2}[\text{ or } y = \frac{3\pi}{2}, x \in]\frac{\pi}{2}, \frac{3\pi}{2}[; \\ -\frac{5}{4} & \text{if } x = \frac{\pi}{2}, y = \frac{\pi}{2} \text{ or } x = \frac{\pi}{2}, y = \frac{3\pi}{2}; \\ \frac{5}{4} & \text{if } x = \frac{3\pi}{2}, y = \frac{\pi}{2} \text{ or } x = \frac{3\pi}{2}, y = \frac{3\pi}{2}; \\ 0 & \text{otherwise} \end{cases} \tag{35}$$

Note that the zero mean value of the numerical solution in the fluid domain is imposed by replacing the first equation in the linear system by

$$\sum_{i,j=\overline{1,N}} [1 - \chi(x_{ij})] \, u_{ij} = 0. \tag{36}$$

In the fluid domain Ω_f, the solution to (33) converges to

$$w(x,y) = \sin x \cos 2y, \text{ where } x \in]\frac{\pi}{2}, \frac{3\pi}{2}[\text{ and } y \in]\frac{\pi}{2}, \frac{3\pi}{2}[, \tag{37}$$

as $\eta \to 0$. Figure 7 displays a numerical solution to this problem with $N = 32$ discretization grid points in each direction and with $\eta = 10^{-8}$. Inside the fluid domain, the solution is close to (37). Outside, it is close to a harmonic function (up to numerical errors). Figure 8 shows the decay of the L^∞ error of the finite-difference solution with respect to the exact solution (37) in the

fluid domain (including the points on the boundary). Two values of η are considered. For $\eta = 10^{-2}$, the error saturates at $h < 0.2$, where $h = 2\pi/N$. For $\eta = 10^{-8}$, the decay approaches the theoretical -2 slope for small h and the saturation is not observed within this range of h, implying that the penalization error is much smaller than the discretization error.

Let us consider a circular fluid domain, with the mask function

$$\chi(x,y) = \begin{cases} 0 & \text{if } r < \pi; \\ \frac{1}{2} & \text{if } r = \pi; \\ 1 & \text{otherwise,} \end{cases} \tag{38}$$

where $r = \sqrt{(x-\pi)^2 + (y-\pi)^2}$. The right-hand side is

$$f(x,y) = \begin{cases} 4\cos 2r + \frac{2\sin 2r}{r} & \text{if } r < \pi; \\ -\frac{1}{2} & \text{if } r = \pi; \\ 0 & \text{otherwise.} \end{cases} \tag{39}$$

The exact solution to the Poisson equation with homogeneous Neumann boundary conditions in this case is

$$w = \cos 2r + \frac{4}{\pi^2}, \text{ where } r < \pi\,, \tag{40}$$

inside the fluid domain embedded in a square computational domain $\Omega = [0, 2\pi] \times [0, 2\pi]$.

We observed that the numerical solution is sensitive to the choice of the linear equation which is replaced with the zero-mean condition. The operator matrix has many small eigenvalues if η is small. Another possibility would be to add the zero-mean condition without removing any of the equations and solve an overdetermined system in the least-square sense (results not shown here). Note that in this case we observed a smooth behavior in the solid domain. Figure 9 shows the solution with the first equation replaced and $\eta = 10^{-8}$, $N = 127$. Figure 10 displays the same solution with the $N^2/2$-th equation replaced, and figure 11 with the $N^2/2 + N/2$-th equation replaced. The solution in the fluid is slightly different in the three cases (and seems to be convergent with η and $h = 2\pi/N$). In the solid domain, a parasite harmonic solution appears, which has a singularity at the point that corresponds to the removed equation. The convergence of the two-dimensional penalized equation for the three above cases is summarized in Figure 12 and shows

first order convergence in all cases. The second order convergence observed in the one-dimensional case (subsec. 2.3) and for the two-dimensional case in the rectangular domain is thus reduced to first order. The reason is that the Cartesian grid introduces a staircase effect and the approximation of the circular mask function reduces to first order. Techniques to obtain higher order for complex geometries (based on interpolation) have been proposed in [16].

5. Conclusions

The volume penalization method to impose homogeneous Neumann boundary conditions has been analyzed by considering the Poisson equation. In one space dimension, the penalized Poisson equation has been solved analytically for a particular right hand side and the penalization error has been determined showing $O(\eta)$ convergence of the solution towards the solution of the exact problem. We also found that no penalization boundary layer is present. This observation is in contrast to what was found for the time-dependent heat equation with Neumann conditions [5] and also for the Poisson equation with Dirichlet boundary conditions [12]. In both cases, there is a penalization boundary layer which becomes thinner for decreasing penalization parameter η and its thickness scales like $O(\sqrt{\eta})$. This implies that only an $O(\sqrt{\eta})$ convergence can be proven [1, 3, 5]. Nevertheless for the penalized Laplace operator with Neumann conditions, the corresponding matrix becomes ill–conditioned and the condition number behaves like $O(1/\eta)$. Thus, special care has to be taken for the numerical solution, as in addition to the singularity of the matrix (the presence of an eigenvalue 0), the linear system becomes stiff.

The performed numerical simulations using second order finite differences yield second order convergence of the solution towards the solution of the Poisson equation, given that the penalization parameter is sufficiently small. Due to the regularity of the exact solution of the penalized equation and the $O(\eta)$ behavior of the penalization error, we anticipate that for higher order numerical methods we will also find second order convergence.

The eigenvalue problem of the penalized Laplace operator with Neumann boundary conditions was also studied in some detail. We found that the spectrum of the penalized operator exhibits two distinct behaviors. The upper part of the spectrum corresponding to the large eigenvalues converges for increasing resolution N to the spectrum of the exact operator ($\propto i^2$).

For the lower part, corresponding to the small eigenvalues, the spectrum exhibits the same power law scaling but the values are multiplied with η and thus converge to zero for $\eta \to 0$. The eigenfunctions in the upper half of the spectrum are non-trivial in either part of the domain. The lower half of the spectrum corresponds to modes that oscillate with the grid frequency in either subdomain. The eigenfunctions corresponding to the upper half of the spectrum of the discrete penalized operator converge to their exact counterparts and we found first order convergence using second order finite differences.

In two space dimensions, we performed numerical simulations for a rectangular geometry for which the grid is aligned with the boundary. In this case we obtained again second order convergence of the numerical solution. For the circular geometry, for which the boundary is not aligned with the Cartesian grid, only first order convergence can be observed which is due to the geometrical error.

An interesting perspective is the extension of the volume penalization to higher order penalization, also called active penalization, using, *e.g.*, smooth extensions of the solution, based for instance on Hermite interpolation, as proposed in [11]. First promising results using active penalization for Navier–Stokes have been presented in [19]. An extension to impose inhomogeneous Neumann conditions has been proposed in [11] for Fourier spectral methods. The underlying idea is to use volume penalization to impose Dirichlet boundary conditions for the derivative and then integrating the equation, which can be easilty done in spectral space.

Acknowledgements

RNVY is grateful to the Humboldt Foundation for its support through a post-doctoral grant. KS thanks the organizers of WONAPDE 2013 for their kind invitation to Concepcion, Chile.

References

[1] P. Angot, C.-H. Bruneau, and P. Fabrie. A penalization method to take into account obstacles in incompressible viscous flows. *Numer. Math.*, **81**, 497–520, 1999.

[2] P. Bochev and R.B. Lehoucq. On the finite element solution of the pure Neumann problem. *SIAM Review*, **47**(1), 50–66, 2005.

[3] G. Carbou and P. Fabrie. Boundary layer for a penalization method for viscous incompressible flow. *Adv. Differential Equations*, **8**(12), 1453–1480, 2003

[4] J. Ferziger and M. Peric. *Numerical methods in fluid dynamics.* Berlin: Springer-Verlag; 1996.

[5] B. Kadoch, D. Kolomenskiy, P. Angot and K. Schneider. A volume penalization method with moving obstacles for Navier–Stokes with advection diffusion equations. *J. Comput. Phys.*, **231**(12), 4365–4383, 2012.

[6] D. Kolomenskiy and K. Schneider. A Fourier spectral method for the Navier–Stokes equations with volume penalisation for moving solid obstacles. *J. Comput. Phys.*, **228**, 5687–5709, 2009.

[7] D. Kolomenskiy, H.K. Moffatt, M. Farge and K. Schneider. Two- and three-dimensional numerical simulations of the clap-fling-sweep of hovering insects. *J. Fluids Struct.*, **27**, 784–791, 2011.

[8] D. Kolomenskiy, T. Engels and K. Schneider. Numerical modelling of flexible heaving foils. *J. Aero-aqua Bio-Mechanisms*, **3**(1), 22–28, 2013.

[9] M. S. Min and D. Gottlieb. On the convergence of the Fourier approximation for eigenvalues and eigenfunctions of discontinuous problems. *SIAM J. Numer. Anal.*, **40**, 2254–2269, 2003.

[10] R. Mittal and G. Iaccarino. Immersed boundary methods. *Annu. Rev. Fluid Mech.*, **37**, 239-261, 2005.

[11] J. Morales, M. Leroy, W. Bos and K. Schneider. Simulation of confined magnetohydrodynamic flows using a pseudo-spectral method with volume penalization. Preprint 07/2012, submitted. (http://hal.archives-ouvertes.fr/hal-00719737)

[12] R. Nguyen van yen, D. Kolomenskiy and K. Schneider. Approximation of the Laplace and Stokes operators with Dirichlet boundary conditions through volume penalization: A spectral viewpoint. *Numer. Math.*, 03/2013, accepted. [arXiv:1206.0002]

[13] C. Peskin. The immersed boundary method. *Acta Numerica*, **11** , 479–517, 2002.

[14] I. Ramière, P. Angot and M. Belliard. A fictitious domain approach with spread interface for elliptic problems with general boundary conditions. *Comput. Methods Appl. Mech. Eng.*, **196**, 766–781, 2007.

[15] I. Ramière, P. Angot and M. Belliard. A general fictitious domain method with immersed jumps and multilevel nested structured meshes. *J. Comput. Phys.*, **225**(2), 1347–1387, 2007.

[16] A. Sarthou, S. Vincent, J.P. Caltagirone and P. Angot. Eulerian–Lagrangian grid coupling and penalty methods for the simulation of multiphase flows interacting with complex objects. *Int. J. Num. Meth. Fluids*, **56**(8), 1093-1099, 2008.

[17] K. Schneider and M. Farge. Decaying two–dimensional turbulence in a circular container. *Phys. Rev. Lett.*, **95**, 244502, 2005.

[18] K. Schneider, S. Neffaa and W.J.T. Bos. A pseudo-spectral method with volume penalisation for magnetohydrodynamic turbulence in confined domains. *Comput. Phys. Comm.*, **182**(1), 2–7, 2011.

[19] D. Shirokoff and J-C. Nave. A Sharp-Interface Active Penalty Method for the Incompressible Navier-Stokes Equations. (Submitted) [arXiv:1303.5681], 2013.

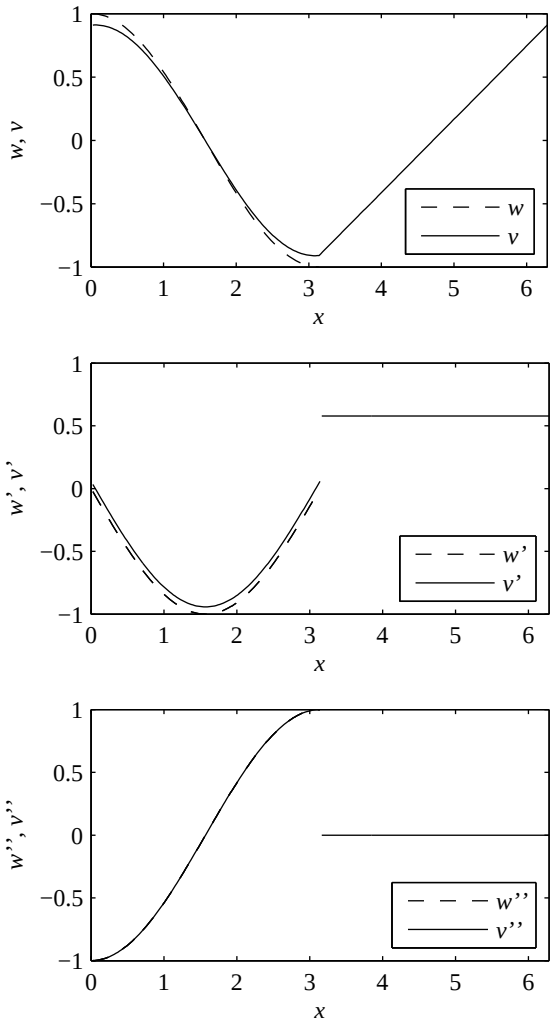

Figure 1: Exact solution of the Poisson equation $w(x)$ and exact solution of the penalized equation $v(x)$ using $\eta = 10^{-1}$, both for $m = 1$ (top). The first (middle) and second (bottom) derivatives are also shown.

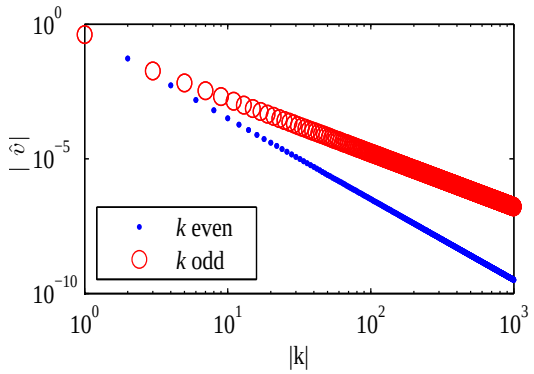

Figure 2: Decay of the Fourier coefficients. Absolute value of the Fourier coefficients of the exact solution of the penalized equation for $m = 1$ using $\eta = 10^{-1}$. The even and odd wavenumbers exhibit different power law behaviors.

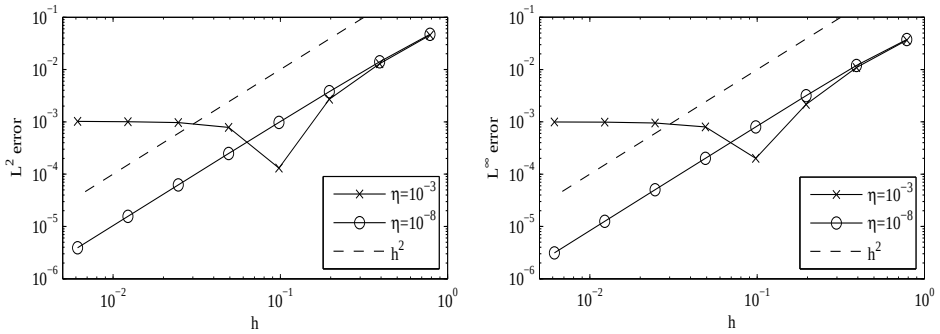

Figure 3: Convergence of the second order finite difference scheme for $m = 1$. The L^2 (left) and L^∞ (right) errors are calculated only in the fluid domain Ω_f.

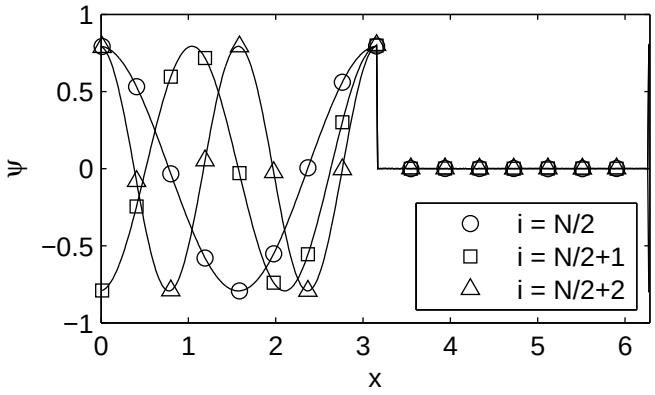

Figure 4: Eigenfunctions number $N/2$, $N/2+1$ and $N/2+2$ of the finite-difference penalized Laplace operator. $N = 512$, $\eta = 10^{-8}$.

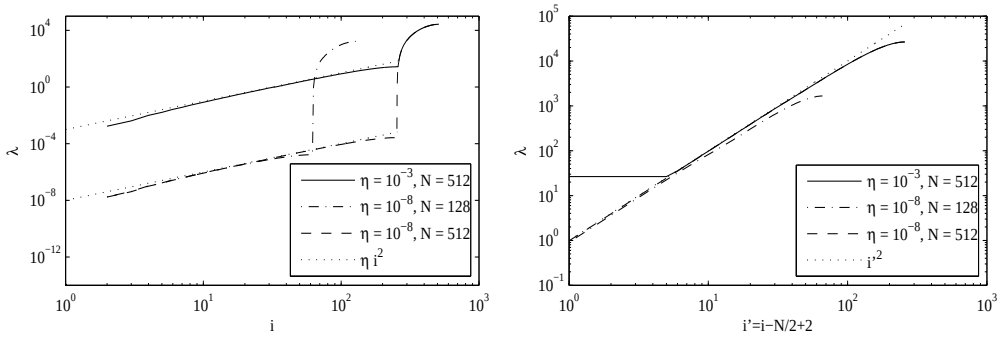

Figure 5: Double-logarithmic plot of the eigenvalues λ_i. Left: Eigenvalues sorted by their magnitude, in the ascending order. The zero eigenvalue is not shown because of the logarithmic scale. Right: Eigenvalues in the upper half of the spectrum correspond to the physically relevant ones.

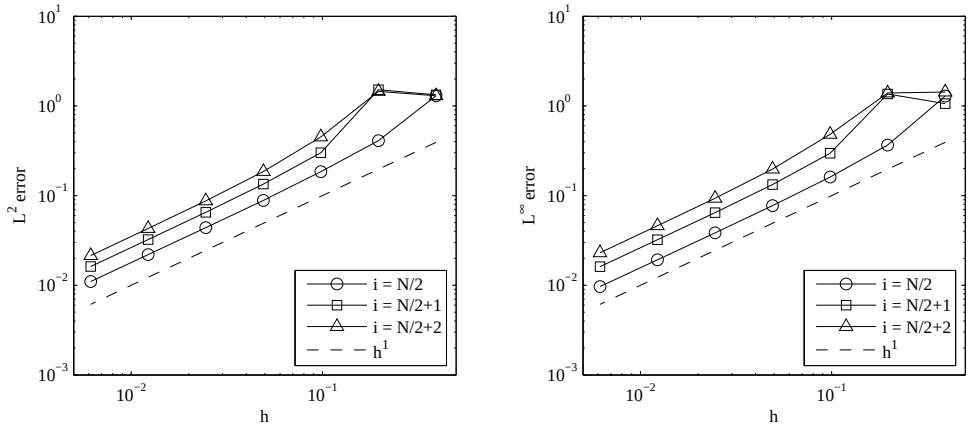

Figure 6: L^2 (left) and L^∞ (right) distance between the $N/2$-th, $N/2+1$-th and $N/2+2$-th eigenfunctions of the discrete penalized Laplace operator and 2nd, 3rd and 4th eigenfunctions of the continuous Laplace operator with Neumann boundary conditions.

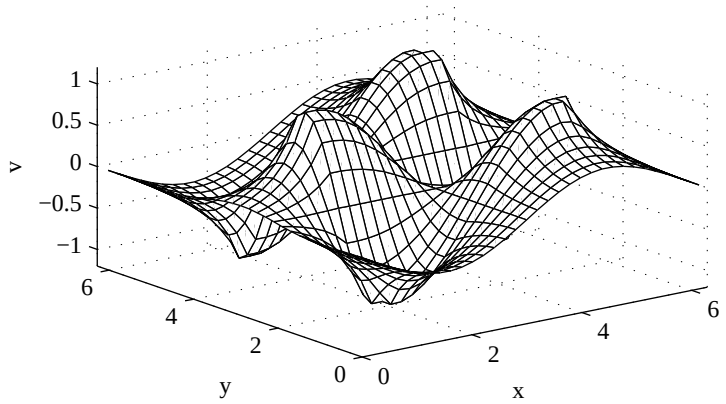

Figure 7: Numerical solution of the two-dimensional penalized equation (33) with $\eta = 10^{-8}$ and $N = 32$ in a rectangular domain.

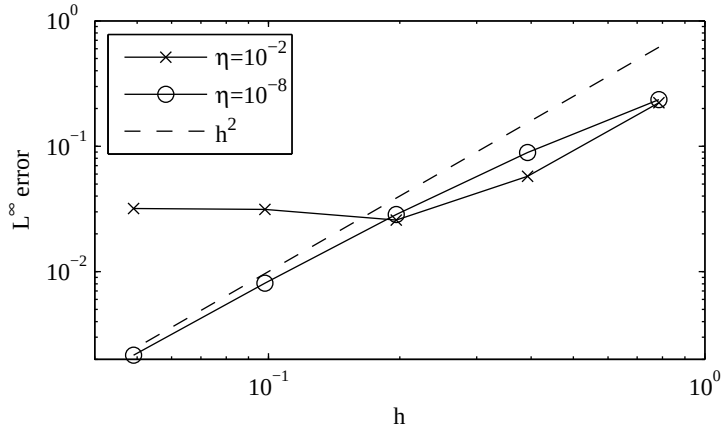

Figure 8: L^∞-error decay of the numerical solution of (33) with respect to the exact solution (37) of the Poisson equation with Neumann boundary conditions in a rectangular domain. $h = 2\pi/N$ is the discretization step size and η is the penalization parameter.

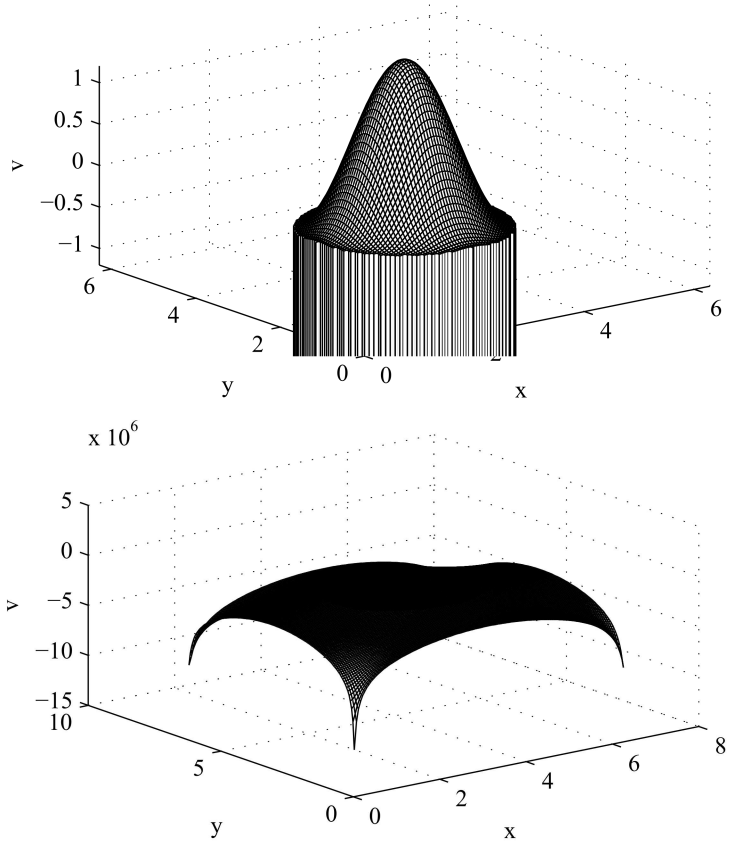

Figure 9: Numerical solution of the two-dimensional penalized equation (33), (38), (39) in a circular domain with $\eta = 10^{-8}$ and $N = 127$, first linear equation replaced with the zero-mean condition. Top: Zoom of solution in the fluid domain. Bottom: Total domain illustrating the singular behavior in the solid domain.

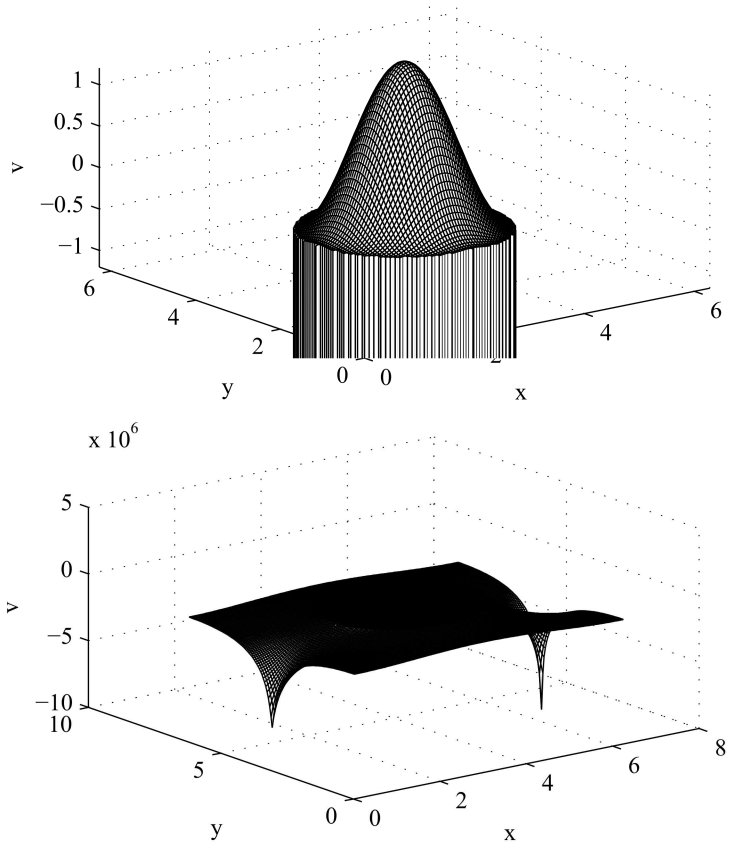

Figure 10: Numerical solution of the two-dimensional penalized equation (33), (38), (39) in a circular domain with $\eta = 10^{-8}$ and $N = 127$, $N^2/2$-th linear equation replaced with the zero-mean condition. Top: Zoom of solution in the fluid domain. Bottom: Total domain illustrating the singular behavior in the solid domain.

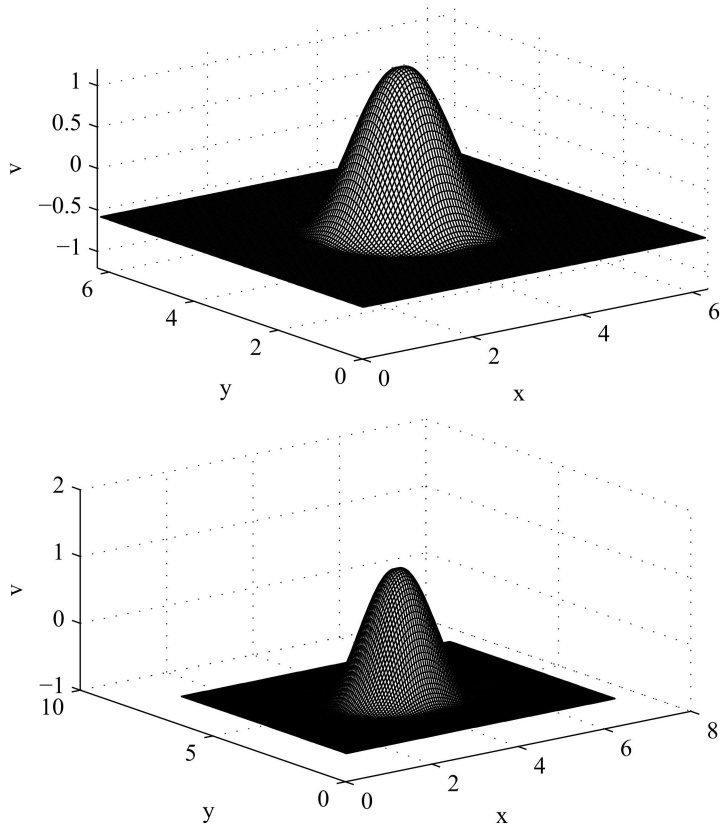

Figure 11: Numerical solution of the two-dimensional penalized equation (33), (38), (39) in a circular domain with $\eta = 10^{-8}$ and $N = 127$, $N^2/2 + N/2$-th linear equation replaced with the zero-mean condition. Top: Zoom of solution in the fluid domain. Bottom: Total domain illustrating the smooth behavior in the solid domain.

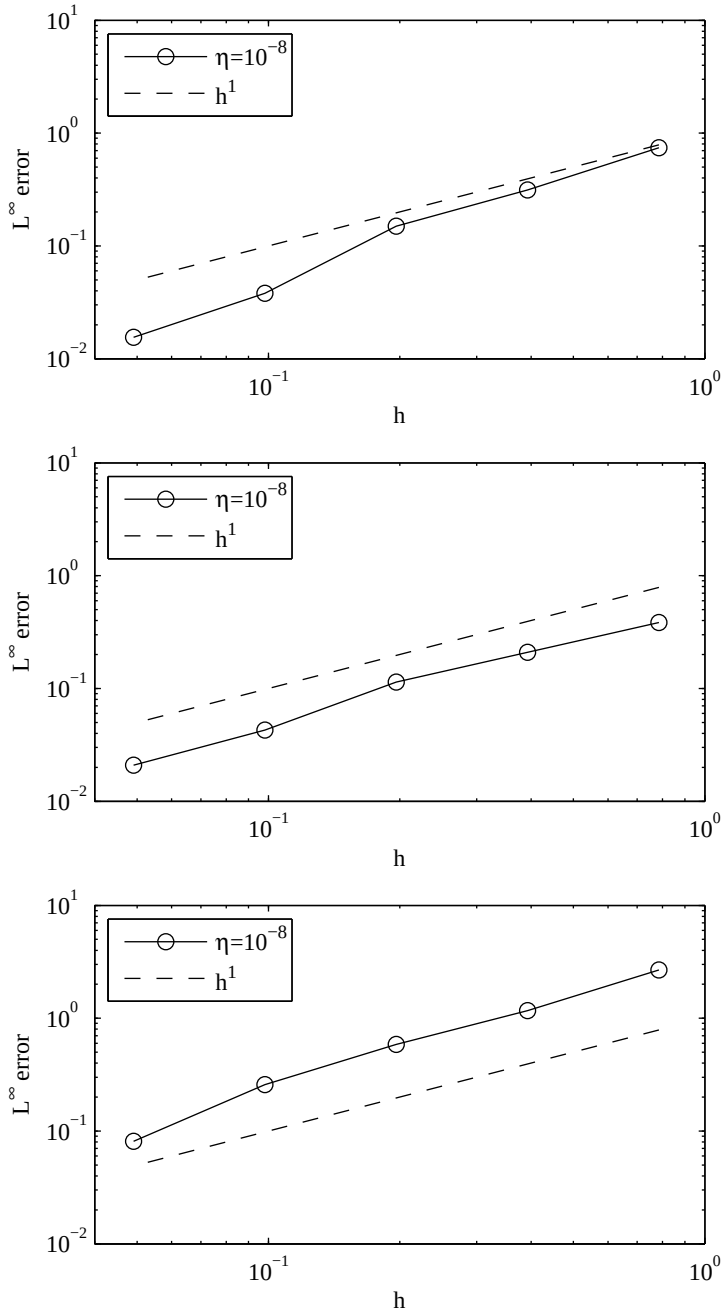

Figure 12: Convergence plots of the two-dimensional penalized equation in a circular domain for the three above cases (see figures 9, 10 and 11, respectively).